New Thermoplastic Segmented Polyurethanes with Hard Segments Derived from 4,4′-Diphenylmethane Diisocyanate and Methylenebis(1,4-phenylenemethylenethio)dialcanols

Anna Kultys,[1] Magdalena Rogulska,[1] Stanisław Pikus[2]

[1]*Department of Polymer Chemistry, Faculty of Chemistry, Maria Curie-Skłodowska University, ul. Gliniana 33, 20–614 Lublin, Poland*
[2]*Department of Crystallography, Faculty of Chemistry, Maria Curie-Skłodowska University, Pl. Marii Curie-Skłodowskiej 3, 20-031 Lublin, Poland*

Received 1 July 2010; accepted 27 December 2010
DOI 10.1002/app.34102
Published online 27 July 2011 in Wiley Online Library (wileyonlinelibrary.com).

ABSTRACT: New thermoplastic poly(ether–urethane)s and poly(carbonate–urethane)s were synthesized by a one-step melt polymerization from poly(oxytetramethylene) diol (PTMO) and poly(hexane-1,6-diyl carbonate) diol (PHCD) as soft segments, 4,4′-diphenylmethane diisocyanate, and 2,2′-[methylenebis(1,4-phenylenemethylenethio)]diethanol, 3,3′-[methylenebis(1,4-phenylenemethylenethio)]dipropan-1-ol or 6,6′-[methylenebis(1,4-phenylenemethylenethio)]dihexan-1-ol as unconventional chain extenders. The effects of the kind and amount of the polymer diol and chain extender used on the structure and properties of the polymers were studied. The polymers were examined by Fourier transform infrared (FTIR) spectroscopy, X-ray diffraction analysis, atomic force microscopy, differential scanning calorimetry, thermogravimetric analysis (TGA), TGA coupled with FTIR spectroscopy, and Shore hardness and tensile testing. The obtained high-molecular-weight polymers showed elastomeric or plastic properties. Generally, the PTMO-based polymers exhibited significantly lower glass-transition temperatures (up to −48.1 vs −1.4°C), a higher degree of microphase separation, and ordering in hard-segment domains in comparison with the corresponding PHCD-based ones. Moreover, it was observed that the polymers with the PTMO soft segments showed poorer tensile strengths (up to 36.5 vs 59.6 MPa) but higher elongations at break. All of the polymers exhibited a relatively good thermal stability. Their temperatures of 1% mass loss were in the range 270–320°C. © 2011 Wiley Periodicals, Inc. J Appl Polym Sci 123: 331–346, 2012

Key words: mechanical properties; polyurethanes; thermal properties

INTRODUCTION

Polyurethanes (PURs), having a wide spectrum of properties, find many industrial applications. They are used as elastomers, foams, coatings, adhesives, fibers, synthetic leathers, and so on and are employed in car industry, building and construction market, shoe manufacturing, medical technology, and so on.[1–3]

Thermoplastic polyurethane elastomers (TPUs) are a very interesting class of these materials. They are block copolymers of the $(A\text{-}B)_n$ type. One block of the polymer chain, called the *soft segment*, imparts elastomeric characteristics to the polymer, whereas the second block, referred to as the *hard segment*, acts as a reinforcing filler and provides physical cross-links by molecular association through hydrogen bonding, performing a role similar to chemical cross-links in rubbers.

In classic TPUs, hard segments are formed by the reaction of short-chain aliphatic diols (chain extenders), mostly butane-1,4-diol (BD), with diisocyanates, mainly 4,4′-diphenylmethane diisocyanate (MDI), whereas soft segments are composed of long-chain diols, such as polyester, polyether, and polycarbonate diols.[1–3] TPUs with polyether soft segments are characterized by better low-temperature properties and hydrolytic resistance than TPUs with polyester soft segments, but they are susceptible to oxidation.[4–9] Improved oxidative resistance[5,10–15] and hydrolytic stability[16–19] are shown by TPUs with polycarbonate soft segments. Because of their combination of excellent biostability and biocompatibility and their high tensile strength and modulus,[10,19–23] they are preferred as biopolymers for long-term implantation.

The influence of the various soft segments on the properties of TPUs containing a hard segment built from conventional aliphatic diols and MDI has been the subject of numerous studies.[1–4,15,20,24–31] Some

Correspondence to: M. Rogulska (mrogulska@umcs.lublin.pl) or A. Kultys (akultys@umcs.lublin.pl).

TABLE I
Designations, Hard-Segment Contents, and η_{red} Values of the SPURs

Diol	SPUR		Soft-segment content (mol %)	Hard-segment content (wt %)		η_{red} (dL/g)	
	PTMO	PHCD		PTMO	PHCD	PTMO	PHCD
E	EE2	EC2	20	72.6	75.5	1.18[a]	—[b]
	EE4	EC4	40	53.6	57.3	1.33	1.15[a]
	EE5	EC5	50	46.0	49.8	1.47	1.30[a]
	EE6	EC6	60	39.5	43.1	1.06	1.36
	EE8	EC8	80	28.7	31.9	0.88	1.00
P	PE2	PC2	20	73.5	76.3	1.35	0.98[a]
	PE4	PC4	40	54.4	58.2	1.80	3.54
	PE5	PC5	50	46.8	50.6	1.94	2.09
	PE6	PC6	60	40.2	43.8	1.71	1.85
	PE8	PC8	80	29.0	32.2	1.10	1.69
H	HE2	HC2	20	75.6	78.3	2.70	3.07
	HE4	HC4	40	56.9	60.6	2.58	2.48
	HE5	HC5	50	49.1	52.9	2.15	2.59
	HE6	HC6	60	42.1	45.8	1.82	2.10
	HE8	HC8	80	30.0	33.4	1.33	2.35

[a] η_{red} values of the soluble fraction.
[b] SPUR insoluble in TChE and other solvents.

investigations have focused on MDI-based TPUs synthesized with other chain extenders. Various aliphatic–aromatic mesogenic diols, including derivatives of biphenyl, benzophenone, and azobenzene, were applied to obtain liquid-crystalline TPUs with polyester or polyether soft segments.[32] TPUs based on poly(oxytetramethylene) diol (PTMO) with improved physical and chemical properties and shape-memory properties compared to conventional TPUs were prepared from 2,2′-[sulfonylbis(1,4-phenyleneoxy)]diethanol, 2,2′-[propane-2,2-diylbis(1,4-phenyleneoxy)]diethanol, and 2,2′-(naphthalene-2,6-diyldioxy)diethanol as chain extenders.[33,34] New-type biodegradable TPUs were synthesized with 2,2′-(methylimino)diethanol[35] or a chain extender based on DL-lactic acid and ethylene glycol[36] and poly(ε-caprolactone) diol as a soft segment. PTMO- and poly(ε-caprolactone) diol–based elastomers produced from various bisphenols were materials with a high thermal stability and improved flame retardancy.[37] Structure–property relationships in poly(ether–urethane)s and/or poly(ester–urethane)s derived from 4,4′-(ethane-1,2-diyl)bis(benzenethioalcanols),[38] 1,3-bis(*N*,*N*′-methyl-*N*,*N*′-2-hydroxyethyl)isophthalamide,[39] 2,2′-(1,4-phenylenedioxy)diethanol, *N*,*N*′-bis(2-hydroxyethyl)terephthalamide, and *N*,*N*′-bis(2-hydroxyethyl)isophthalamide[40] have also been studied. The unconventional aliphatic chain extender *cis*-but-2-ene-1,4-diol was also used to obtain poly(carbonate–urethane)s as new potential biomedical materials.[41]

The main purpose of this work was to study the effect of polyether and polycarbonate soft segments on the morphology, crystallinity, and some physicochemical, thermal, and mechanical properties of new thermoplastic segmented polyurethanes (SPURs). The SPURs were synthesized from 20 to 80 mol % PTMO, with a number-average molecular weight of 1000, and poly(hexane-1,6-diyl carbonate) diol (PHCD), with a number-average molecular weight of 860, as soft segments; MDI; and unconventional aliphatic–aromatic chain extenders containing sulfide linkages in their structure: 2,2′-[methylenebis(1,4-phenylenemethylenethio)]diethanol (diol E), 3,3′-[methylenebis(1,4-phenylenemethylenethio)]dipropan-1-ol (diol P), or 6,6′-[methylenebis(1,4-phenylenemethylenethio)]dihexan-1-ol (diol H). In this article, we also discuss the influence of the chain extender structure (methylene group content) on the properties of the poly(ether–urethane)s with a PTMO soft segment and poly(carbonate–urethane)s with a PHCD soft segment. Additionally, we raise the problem of the effect of sulfide linkages on the thermal stability of the synthesized SPURs and propose the mechanism of decomposition of the unconventional hard segment.

Because the structure of the newly obtained SPURs incorporated sulfur atoms, they could exhibit improved antibacterial activity and adhesive properties.[42,43] The related studies will be presented in a separate publication.

With regard to comparison, this work also gives a detailed characterization of the newly obtained regular (hard-segment type) PURs based on diol E, P, and H and MDI and the thermal and mechanical properties of the PURs obtained without a chain extender, that is, from MDI and PTMO or PHCD.

For SPURs, the system of designation was as follows (see Table I): XYZ, where X is the abbreviation of the diol used as a chain extender (E, P, H), Y

refers to a polyether (E) or polycarbonate (C) soft segment, and *Z* represents the soft-segment content in the polymer (e.g., 2 stands for 20 mol %). For example, EE2 is a polymer prepared from diol E and 20 mol % PTMO.

EXPERIMENTAL

Materials

The diols E (mp = 77–78°C), P (mp = 71–72°C), and H (mp = 67–68°C) were obtained by the condensation reaction of (methylenedi-1,4-phenylene)dimethanethiol with 2-chloroethanol, 3-chloropropan-1-ol, and 6-chlorohexan-1-ol, separately. The general procedure for the synthesis of diols by this method was as follows. Dithiol (0.12 mol) was dissolved in 500 mL of a 10% aqueous solution of sodium hydroxide, and the resulting solution was warmed to about 60°C. Then, a solution of a suitable chloroalcanol (0.25 mol) in 10 mL of ethanol was added dropwise under vigorous stirring for about 5 min. The reaction mixture was heated and stirred in a boiling water bath for 1 h. After some time, the product of condensation separated as a colorless oil. After the reaction was over, the reaction mixture was cooled, and the solidified product was collected by filtration, washed thoroughly with water, and dried in air (yield = 86–96%). The crude compounds were recrystallized twice from benzene (yield = 58–62%).[44]

Before being used, PTMO and PHCD, from Aldrich (Milwaukee, WI), were heated at 90°C *in vacuo* for 10 h. MDI (98%), from Sigma-Aldrich (Steinheim, Germany), and dibutyltin dilaurate, from Merck-Schuchardt (Hohenbrunn, Germany), were used as received. The polymerization solvent, *N,N*-dimethylformamide (DMF), with a water content of less than 0.02%, was purchased from Merck (Darmstadt, Germany) and was used as received. The solvent was stored over activated 3- to 4-Å molecular sieves.

Measurements

The reduced viscosities (η_{red}'s; dL/g) of 0.5% polymer solutions in 1,1,2,2-tetrachloroethane (TChE) were measured in an Ubbelohde viscometer (Gliwice, Poland) at 25°C. Fourier transform infrared (FTIR) spectra were obtained in transmission mode with a PerkinElmer 1 725 X FTIR spectrophotometer with thin films or KBr disks (Beaconsfield, United Kingdom). Elemental analysis was performed with a PerkinElmer CHN 2400 analyzer. Thermogravimetric analysis (TGA) was performed on a MOM 3 427 derivatograph (Paulik, Paulik, and Erdey, Budapest, Hungary) at a heating rate of 10°C/min in air; Al_2O_3 was used as a standard substance. TGA coupled with FTIR spectroscopy (TGA–FTIR) was carried out with a Netzsch TG 209 thermal analyzer (Günzbung, Germany; heating range = 20–1000°C, heating rate = 10°C/min, sample weight ≈ 10 mg, argon flow = 20 mL/min) and a Bruker FTIR IFS66 spectrophotometer. Differential scanning calorimetry (DSC) thermograms were obtained with a Netzsch 204 calorimeter in the range −100 to 200°C. The reported transitions were taken from the first and second heating scans. The scans were performed at a heating/cooling rate of 10°C/min under a nitrogen atmosphere (flow = 30 mL/min). Sample weights of about 10 mg were used. The glass-transition temperatures (T_g's) for the polymer samples were taken as the inflection point on the curves of the heat-capacity changes. The melting temperatures (T_m's) were read at endothermic peak maxima. X-ray diffraction (XRD) measurements were performed with a DRON-3 X-ray apparatus (St. Petersburg, Russia) with a copper tube and nickel filter. The XRD patterns of the investigated samples were obtained by measurement of the number of impulses within a given angle over 10 s. The measurements were taken every 0.02°. The XRD patterns were analyzed by the WAXSFIT computer program (Norwalk, Connecticut, USA).[45] The program resolved a diffraction curve on the diffraction peaks and amorphous halo; this allowed estimation of the crystallinity degree. Atomic force microscopy (AFM) was carried out on a Multimode microscope (Digital Instruments, CA) in tapping mode in air. The phase data were recorded simultaneously. Silicon probes were used (TESP, Digital Instruments) with a nominal spring constant of 20–100 N/m. To compare the structures of all of the investigated samples, the imaging parameters were kept constant. Phase images at a 1-μm scan size were obtained with a hard tapping technique. Two types of specimens were used: the cuttings from crude polymers after their 1-month conditioning at room temperature and freshly cast films. The films were made with a 5 wt % solution of polymer in TChE. Two drops of each solution were deposited on clean glass discs and dried for 24 h in air at 25°C and then at 40°C *in vacuo* to completely remove the solvent. The hardness of the polymers was measured by the Shore A/D method on a Zwick 7206/H04 hardness tester (Germany) at 23°C. The values were taken after 15 s. Tensile testing was performed on a TIRA Test 2200 tensile testing machine according to Polish Standard PN-81/C-89034 (EN ISO Standard 527-1 : 1996 and 527-2 : 1996) at a speed of 100 mm/min at 23°C; tensile test pieces 1 mm thick and 6 mm wide (for the section measured) were cut from the pressed sheet. Molding was done with a Carver hydraulic press at 65–170°C under a pressure of about 10–30 MPa.

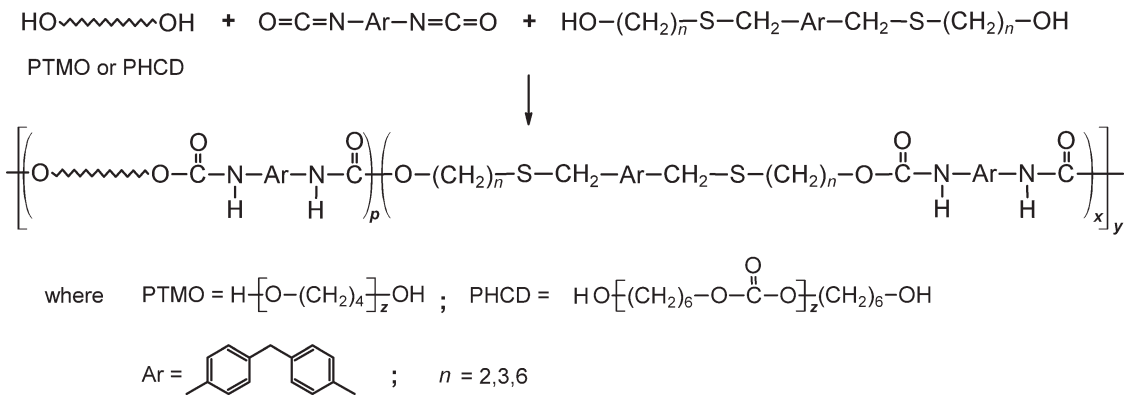

Scheme 1 Reaction scheme for synthesis of the SPURs.

Polymer synthesis

Regular PURs were prepared by the solution polymerization of an equimolar amount (0.01 mol) of diol E, P, or H and MDI (DMF, concentration ≈ 20 wt %); this was carried out under dry nitrogen for 4 h at 85°C in the presence of a catalytic amount of dibutyltin dilaurate. The polymer precipitated and then washed with methanol was dried at 100°C *in vacuo*. The yield was 91–93%.

FTIR (KBr, cm^{-1}): 1730, 1704–1703 (nonbonded and bonded C=O stretching), 1528–1524 (N—H bending), 3402–3390 (N—H stretching of the urethane group), 2923–2915 and 2854–2845 (asymmetric and symmetric C—H stretching, respectively, of CH_2), 1598–1596 (benzene ring).

Elemental analysis

ANAL. PUR from diol E: Calcd for $C_{34}H_{34}N_2O_4S_2$: C, 68.18%; H, 5.72%; N, 4.70%. Found: C, 68.00%; H, 5.64%; N, 5.00%.

ANAL. PUR from diol P: Calcd for $C_{36}H_{38}N_2O_4S_2$: C, 68.96%; H, 6.10%; N, 4.49%. Found: 68.91%; H, 6.04%; N, 4.72%.

ANAL. PUR from diol H: Calcd. for $C_{42}H_{50}N_2O_4S_2$: C, 70.93%; H, 7.09%; N, 3.96%. Found: C, 70.70%; H, 6.97%; N, 4.20%.

SPURs were prepared by a one-step melt polymerization process from MDI; diol E, P, or H; and 20, 40, 50, 60 or 80 mol % PTMO or PHCD at an NCO/OH molar ratio of 1.

The general procedure for the synthesis of SPURs by this method was as follows. The diol E, P, or H and PTMO or PHCD (0.01 mol together) were heated under dry nitrogen to 110°C in an oil bath. MDI (0.01 mol) was added to melted and mixed dihydroxy compounds, and the reaction was continued until the viscosity increase made stirring impossible. Then, the reaction temperature was gradually raised to 130°C, and the formed colorless, rubberlike, or hard product was conditioned at this temperature for 2 h.

Under the same conditions used for the SPURs, the syntheses of the PURs obtained without a chain extender were carried out.

FTIR of the PTMO-based SPURs (film, cm^{-1}): 1538–1529 (N—H bending), 3322–3306 (N—H stretching of the urethane group), 1733–1728 and 1708–1703 (nonbonded and bonded C=O stretching, respectively, of the urethane group), 1111–1103 (C—O stretching of the ether group), 2942–2934 and 2862–2856 (asymmetric and symmetric C—H stretching, respectively, of CH_2), 1599–1598 (benzene ring).

FTIR of the PHCD-based SPURs (film, cm^{-1}): 1533–1530 (N—H bending), 3349–3331 (N—H stretching of the urethane group), 1743–1706 (C=O stretching of the urethane and carbonate groups), 1261–1256 (C—O stretching of the carbonate group), 2940–2934 and 2863–2857 (asymmetric and symmetric C—H stretching, respectively, of CH_2), 1598–1597 (benzene ring).

RESULTS AND DISCUSSION

Polymer synthesis and characterization

The new regular (hard-segment-type) thermoplastic PURs were synthesized by a step-growth polymerization of the aliphatic–aromatic diol E, P, or H with MDI. Their chemical structures were confirmed by FTIR spectroscopy and elemental analysis. All of these polymers were colorless solids and were insoluble in common organic solvents at room temperature. For the polymers derived from diol P and H and soluble in TChE, the η_{red} values were determined, which equaled 0.23 and 0.55 dL/g, respectively.

The related thermoplastic SPURs were obtained, according to Scheme 1, by partial replacement of diol E, P, or H by 20–80 mol % PTMO or PHCD. Table I gives the designations, hard-segment contents, and η_{red} values.

The resulting SPURs were colorless solids. The η_{red} values determined for polymers soluble in

TChE, ranging from 0.88 to 3.54 dL/g (see Table I), pointed to their high molecular weights. On the basis of the obtained data, it could be said that the η_{red} values increased with the increase of aliphatic length in the chain extender used.

All of the PTMO-based SPURs (except EE2) were completely soluble in TChE, DMF, *N*,*N*-dimethylacetamide, *N*-methyl-2-pyrrolidone, and tetrahydrofuran at room temperature. On the whole, the PHCD-based SPURs exhibited worse solubility, especially those containing fewer PHCD soft segments.

The chemical structures of the SPURs were examined by FTIR spectroscopy. All of the spectra exhibited significant absorptions of the urethane group, benzene ring, methylene group, and carbonate or ether group. PURs require a precise analysis of the carbonyl stretching region, which gives some information about their order of hard domains or degree of microphase separation.[25,39]

The spectra of the regular PURs showed two weakly separated bands at 1730 cm^{-1} (less intensive) and 1704–1703 cm^{-1}, characteristic of nonbonded and H-bonded urethane carbonyl groups, respectively; this is shown as an example for the polymer from diol E in Figure 1. For the PTMO-based SPURs, two bands at 1733–1728 and 1708–1703 cm^{-1} were also observed, but in this case, the less intensive was the latter, which corresponded to the H-bonded carbonyl groups in ordered hard domains.[28] The intensity of this band decidedly diminished for polymers with a high PTMO content (60 and 80 mol %); this was connected with a reduction of ordered hard-segment domains in the polymer. A smaller difference in the intensity of the H-bonded band compared to the nonbonded band in polymers derived from diol H compared to those derived from diols E and P with the same soft-segment content (similar hard-segment content) indicated a higher degree of microphase separation in diol H-derived polymers, which was subsequently confirmed by DSC studies. Figure 1 shows the spectra of the polymers HE5, HE6, HE8, and EE6.

In the spectra of the PHCD-based SPURs, a carbonyl band at 1743–1706 cm^{-1} was observed; it became ever sharper with the increase of the soft-segment content. The spectra of the polymers with 20 mol % PHCD content exhibited non-hydrogen-bonded urethane carbonyl stretching at 1734–1731 cm^{-1} and H-bonded urethane carbonyl stretching at about 1706 cm^{-1} (shoulder), whereas carbonate carbonyl stretching was almost invisible. In the spectra of the remaining SPURs, the absorption of carbonate carbonyl at 1743–1739 cm^{-1} predominated, which masked the non-hydrogen-bonded urethane carbonyl stretching,[28] whereas the H-bonded urethane carbonyl stretching disappeared with the increase of the soft-segment content.

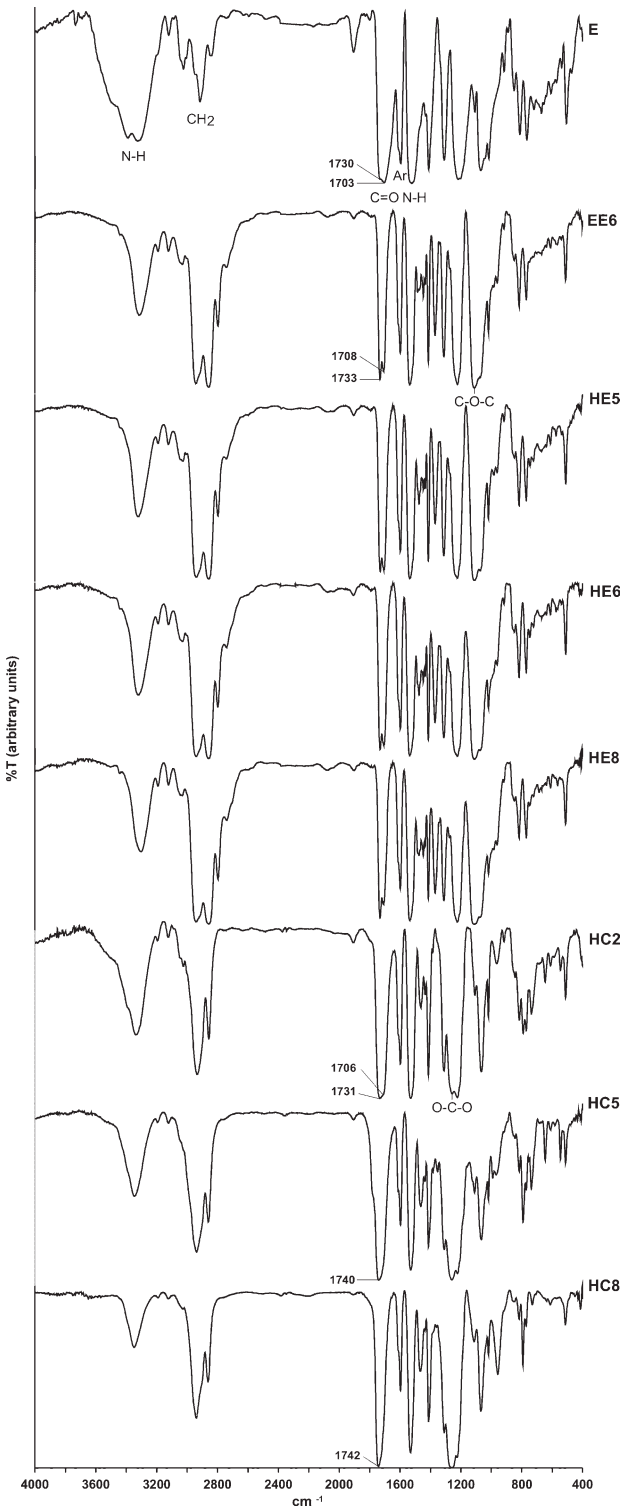

Figure 1 FTIR spectra of the SPURs based on PTMO and PHCD and (E) regular PUR from diol E.

The absence of distinct H-bonded urethane carbonyl stretching absorption in the PHCD-based SPURs indicated a much lower degree of microphase separation in these polymers in comparison with the PTMO-based analogs. As an instance,

TABLE II
Thermal Properties of the Regular PURs

	DSC				TGA in air (°C)				
	T_g (°C)		T_m (°C)	ΔH (J/g)					
Diol	I[a]	II[a]	I[a]	I[a]	T_1	T_5	T_{10}	T_{50}	T_{max}[b]
E	70.5	72.5	129.9, 153.3	37.0	255	295	320	460	320, 350, 530, 660
					295[c]	333[c]	344[c]	380[c]	373[c], 521[c]
P	43.9	63.8	117.1, 124.5	33.5	280	315	325	465	355, 365, 520, 680
H	19.3	44.8	123.9	49.5	265	315	330	415	350, 385, 520, 680

[a] I and II, first and second heating scans, respectively.
[b] From the TG (T_1, T_5, T_{10}, T_{50}) or DTG (T_{max}) curves.
[c] TGA data obtained in argon during TGA–FTIR analysis.

Figure 1 presents the spectra of polymers HC2, HC5, and HC8.

Thermal properties

The thermal behavior was investigated by means of DSC and TGA for all of the synthesized polymers and PTMO and PHCD and by means of TGA–FTIR for selected polymers.

DSC

The obtained numerical data for all of the polymers [definite T_g, T_m, and heat of melting (ΔH) values] are summarized in Tables II–IV, whereas the DSC curves of all of the regular PURs and the SPURs based on PHCD and PTMO are presented in Figure 2.

The DSC curves of the regular PURs from the first heating scans showed glass transitions in the range 19.3–70.5°C and one or two endothermic peaks with maxima in the range 117.1–153.3°C, whereas those from the second heating scans showed only a glass transition. The lack of exothermic and endothermic peaks in the second heating scans pointed to a relatively low tendency for forming ordered structures in the obtained regular PURs. The highest ΔH value and a sharp and high endothermic peak observed for the polymer from diol H suggested its highest degree of ordering. It was also found that an

TABLE III
Thermal Properties of the PTMO-Based SPURs and the PUR Obtained Without the Use of a Chain Extender (PTMO+MDI) and PTMO

	DSC				TGA in air (°C)				
	T_g (°C)		T_m (°C)	ΔH (J/g)					
Polymer	I[a]	II[a]	I[a]	I[a]	T_1	T_5	T_{10}	T_{50}	T_{max}[b]
EE2	26.3	28.3	110.7, 158.6	4.3	275	305	320	430	325, 410
EE4	—16.8	−0.5	73.9, 97.1	18.3	295	320	340	420	360, 410
EE5	−29.3	−16.2	52.9, 93.4	10.1	300	325	340	420	360, 410
					320[c]	337[c]	348[c]	399[c]	364[c], 399[c]
EE6	−31.2	−22.6	66.7, 84.8	10.6	290	330	350	415	360, 405
EE8	−40.1	−37.7	65.3	4.3	290	325	350	400	360, 400
PE2	18.9	20.6	62.2, 102.3	12.9	285	310	325	410	350, 380
PE4	−19.1	−4.1	69.8, 86.5	21.2	305	330	345	410	355, 400
PE5	−35.3	−18.0	62.9, 87.6	17.2	310	330	350	410	355, 400
PE6	−35.9	−25.1	65.3, 80.3	16.6	310	330	340	405	355, 400
PE8	−44.6	−41.0	69.2	6.2	305	340	350	405	350, 410
HE2	6.0	15.2	66.0, 113.4	28.8	300	320	325	410	345, 380
HE4	−20.8	−10.4	57.9, 100.2	25.2	300	325	340	410	350, 400
HE5	−33.6	−19.4	60.3, 97.5	20.4	315	330	340	410	360, 410
HE6	−38.4	−25.6	62.1, 89.5	17.9	310	330	350	410	360, 405
HE8	−48.1	−40.6	60.5, 70.5	8.0	290	330	345	405	360, 400
PTMO+MDI	−49.7	−50.1	Broad endotherm	5.9	290	330	350	410	410
PTMO	−76.6	−77.6	15.5, 30.4 (0.5, 23.1)[d]	119.6 (107.9)[d]	175	235	260	370	315, 410

[a] I and II, first and second heating scans, respectively.
[b] From the TG (T_1, T_5, T_{10}, T_{50}) or DTG (T_{max}) curves.
[c] TGA data obtained in argon during TGA–FTIR analysis.
[d] The values obtained from the second heating scan.

TABLE IV
Thermal Properties of the PHCD-Based SPURs and the PUR Obtained Without the Use of a Chain Extender (PHCD+MDI) and PHCD

	DSC								
	T_g (°C)		T_m (°C)	ΔH (J/g)	TGA in air (°C)				
Polymer	I[a]	II[a]	I[a]	I[a]	T_1	T_5	T_{10}	T_{50}	T_{max}[b]
EC2	47.0	49.3	148.9	18.7	270	305	320	380	365
EC4	28.6	29.6			275	310	320	370	360
EC5	20.8	21.4			285	310	325	370	360
					295[c]	326[c]	336[c]	370[c]	363[c]
EC6	16.2	15.8			280	315	325	370	360
EC8	4.2	4.1			280	310	320	360	360
PC2	45.4	43.5			280	320	330	390	360
PC4	25.4	26.2			280	315	330	380	360
PC5	18.1	19.0			285	320	340	370	370
PC6	12.2	13.2			285	320	330	370	365
PC8	−0.6	2.9			290	320	335	370	370
HC2	30.6	31.4			310	325	340	390	365
HC4	17.8	19.2			290	325	335	380	365
HC5	14.3	14.4			300	325	335	370	370
HC6	8.4	9.6			290	325	335	370	370
HC8	−1.4	−1.4			290	320	335	370	370
PHCD+MDI	−1.4	−3.7			280	320	340	370	370
PHCD	−68.6	−63.4	10.4, 30.5 (31.0)[d]	55.5 (37.2)[d]	165	235	275	345	360

[a] I and II, first and second heating scans, respectively.
[b] From the TG (T_1, T_5, T_{10}, T_{50}) or DTG (T_{max}) curves.
[c] TGA data obtained in argon during TGA–FTIR analysis.
[d] The values obtained from the second heating scan.

increase of methylene group content in the diol component caused the decrease of polymer T_g's.

The DSC curves of the PHCD-based SPURs (except for polymer EC2 from the first heating scan) exhibited only a glass transition; this pointed to the amorphous structure of these polymers. In the case of polymers EC2, PC2, and HC2 (see Fig. 2), the first heating scans showed a relaxation peak superimposed on the glass transition. However, the second heating scans of these SPURs exhibited the glass transition in a normal shape. These endothermic peaks resulted from the relaxation of the enthalpy occurring during the storage of amorphous polymers in a temperature not much lower than the temperature of the glass-transition region. From a comparison of the values of the T_g of PHCD (−68.6°C) and those of the obtained polymers (−1.4 to 47.0°C), it appeared that in all of these polymers, there was a very weak microphase separation, which, however, improved with the increase of the soft-segment content. This tendency was observed in each series of the PHCD-based SPURs.

The DSC curves of all of the PTMO-based SPURs from the first heating scans showed, apart from the glass transition in the range of −48.1 to 26.3°C, one or two endothermic peaks with maxima at 52.9–158.6°C connected with the hard-segment melting. The peaks at lower temperatures could be ascribed to the melting of less ordered structures, but those at higher temperatures to were ascribed to greater ordered structures, including semicrystalline ones. In contrast, the DSC curves from the second heating scans exhibited only a glass transition (as in the case of the regular PURs), shifted to higher temperatures. A shift of the glass transition to higher temperatures was caused by an increase in the mutual miscibility of the soft and hard segments during the first heating. For each series of the polymers in both heating scans, the increase in PTMO content caused a decrease in T_g, which showed an increase of the degree of microphase separation. A rapid drop in T_g followed at a content of 40 mol % PTMO (hard-segment content ≈ 55 wt %).

When the T_g of the SPURs and the respective soft segments were compared, it could be said that the considerably higher degree of microphase separation was shown by the PTMO-based SPURs. A much weaker microphase separation observed for the PHCD-based SPURs was the result of a stronger interaction of hard-segment urethane groups with carbonate groups of oligocarbonate chains compared to that with ether groups of oligoether chains.

For the SPURs, both with a PTMO and PHCD soft segment, the ability of microphase separation was dependent not only on the soft-segment content but also on the kind of chain extender used, and it grew with the increased methylene group content in the chain extender structure (the higher the molar mass

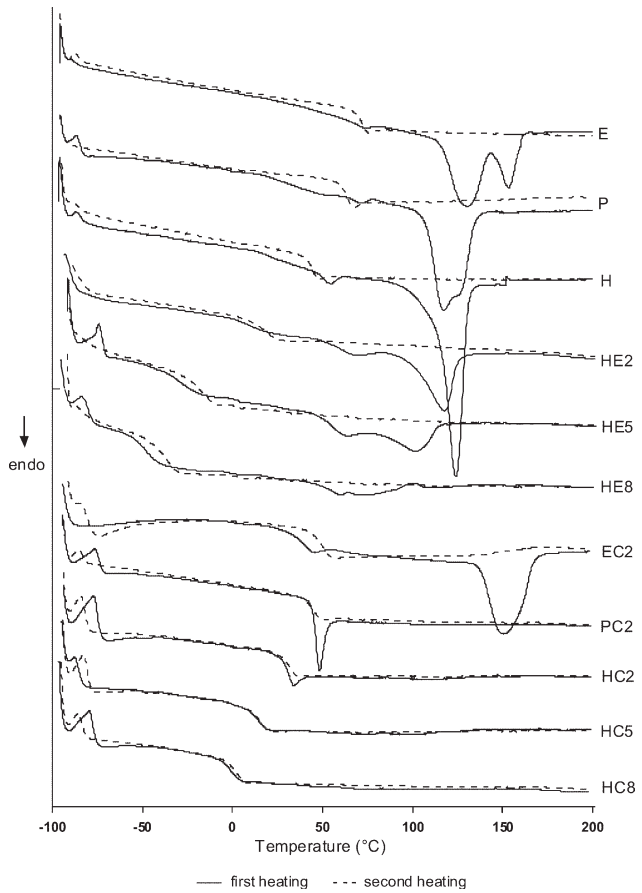

Figure 2 DSC curves of the SPURs based on PTMO and PHCD and the regular PURs: (E) from diol E, (P) from diol P, and (H) from diol H.

of the hard segment was, the better the microphase separation was).

TGA

The decomposition process of all of the polymers was performed in oxidative atmosphere (air). Performing the measurements in air is important for the determination of the acceptable temperature of the processing of thermoplastic materials (e.g., injection molding, extrusion, pressing). The TGA studies were also carried out in an inert atmosphere (argon) for two selected SPURs with PTMO and PHCD soft segments (EE5 and EC5) and for the corresponding regular PUR (from diol E). The numerical data are given in Tables II–IV.

In an oxidative atmosphere, the decomposition of both the regular PURs and SPURs was a multistage process. In the case of the regular PURs, the differential thermogravimetric (DTG) curves showed two relatively sharp overlapping peaks with maxima in the range 320–385°C; these were connected with decomposition of the urethane and sulfide bonds. After this region, there was a peak at 520–530°C, associated with the aromatic content in the polymer,[46] and then a very wide peak at 660–680°C, which corresponded to the oxidation of the char formed in the previous stages. DTG curves of the SPURs with a PTMO soft segment exhibited in the region 325–410°C two overlapping peaks, the former connected to the decomposition of the hard segment and the latter connected to the soft segment.[47,48] With the drop in the hard-segment content, a transformation of the first peak was observed, beginning as early as EE4, PE4, and HE4, into a less and less visible shoulder, and ending in its total disappearance for sample suitable polymer containing no chain extender. In this region, the DTG curves of the SPURs with a PHCD soft segment exhibited only one peak, with a maximum at 360–370°C. This indicated that the decomposition of the PHCD soft segment occurred in the temperature range of the main decomposition of the hard segments. Further decomposition stages of the PURs had a similar course as the regular PURs; hence, in Tables III and IV, the temperature of the maximum rate of mass loss (T_{max}) values are given for the region 325–410°C.

As can be seen from the TGA data in Tables II–IV, the SPURs generally showed higher temperatures of 1, 5, and 10% mass loss from the TG curve (T_1, T_5, and T_{10}, respectively) than the comparable regular PUR ones (T_1 = 270–315 vs 255–280°C; T_5 = 305–340 vs 295–315°C; T_{10} = 320–350 vs 320–330°C). On the other hand, higher temperatures of 50% mass loss from the TG curve (T_{50}) values were observed for the regular PURs, especially for those with shorter methylene sequences, this being the result of a higher content of benzene rings in the structure of these polymers. The lowering of the hard-segment content in the SPURs caused some reduction in T_{50}, with the EE series having the greatest effect in this respect.

During the decomposition of regular PUR from diol E and the SPURs (EE5 and EC5), in an inert atmosphere (argon), no last step connected with the oxidation of unvolatile residue was observed, whereas earlier stages had a similar course to that in the oxidative atmosphere. Only for the regular PUR in the range 320–385°C was there one peak instead of two. The data in Tables II–IV show that higher T_1, T_5, and T_{10} values were received for the analysis carried out in argon. Figure 3 shows the DTG and thermogravimetric (TG) curves of the SPURs EE5 and EC5 and the regular PUR from diol E in argon.

The TGA data analysis also showed that a somewhat better thermal stability, both in air and in argon, was exhibited by the PTMO-based polymers.

TGA–FTIR

For a better explanation of the process of decomposition and identification of the resulting volatile

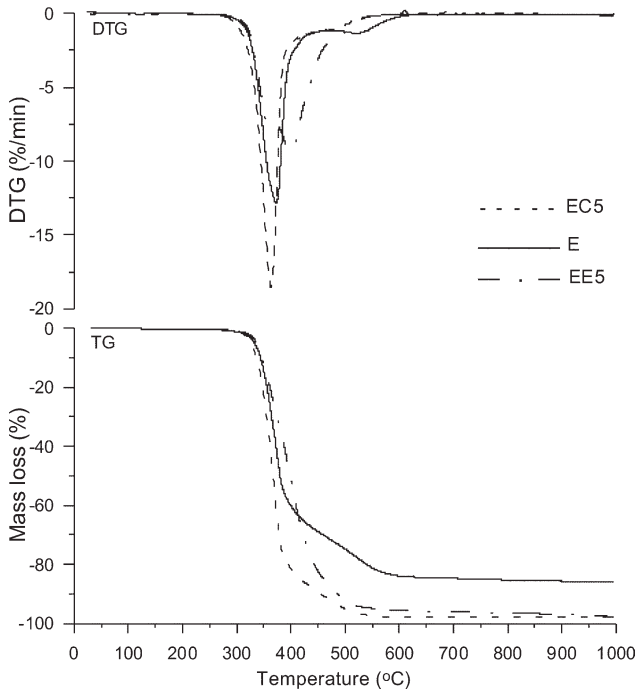

Figure 3 DTG and TG curves of the SPURs EE5 and EC5 and (E) regular PUR from diol E obtained in argon.

products, the TGA–FTIR method was applied. In this article, the analysis was performed for polymers based on diol E, that is, the regular PUR and chosen SPURs (EE5 and EC5).

The FTIR spectra of the decomposition products of the polymers at the maximum rate of mass loss are shown in Figure 4. The spectra recorded during the first decomposition stage for the regular PUR (373°C), EE5 (364°C), and EC5 (363°C) exhibited a very strong double absorption band at 2071 and 2049 cm^{-1}, characteristic of asymmetric and symmetric C=O stretching in carbonyl sulfide,[49] and strong bands at 2360–2331 and 668 cm^{-1}, attributed to carbon dioxide. Moreover, the spectra showed a band at 3900–3350 cm^{-1}, which could have been related to O—H stretching vibrations from both water and alcohols. The presence of alcohols confirmed the C—OH stretching vibration bands at 1060–1040 cm^{-1}. A weak band at 3370 cm^{-1}, which could have been attributed to N—H stretching vibrations from amines was found only for the regular PUR and EE5, and so the band at 1260 cm^{-1} could have been related to C—N stretching vibration from amines (for the regular PUR and EE5) or C—O stretching vibration from the carbonate group (for EC5). The appearance of an additional band at 916–912 cm^{-1} may have pointed to the existence of ethylene oxide. Carbonyl bands at 1740 and 1709 cm^{-1} (for the regular PUR and EE5) and at 1750 cm^{-1} (for EC5) were also present. Moreover, in the case of polymers EE5 and EC5, bands at 2938–2935 and 2875–2862 cm^{-1} could be found, which is typical of asymmetric and asymmetric C—H stretching vibrations of methylene and methyl groups. There was also a relatively strong band at 1113 cm^{-1} (for EE5) or a very weak band at 1130 cm^{-1} (for EC5) associated with the C—O stretching of the ether group from aliphatic ethers. In the case of the regular PUR, the bands at 3013–2910 cm^{-1} pointed to the presence of aromatic compounds (=C—H stretching vibration), methylene and methyl groups (asymmetric C—H stretching vibration), and the epoxide ring (C—H stretching vibration).

In the EE5 spectrum at the maximum rate of mass loss for the second stage of decomposition (399°C), an increase in the intensity of bands attributed to the C—H stretching vibration of methylene and methyl groups and C—O stretching of the ether group, a band disappearance for carbonyl sulfide, and a decrease in the band intensity for carbon dioxide were observed. Besides, a clear absorption of the carbonyl group in aldehydes at 1750 and 1734 cm^{-1} was observed. The presence of aldehydes was confirmed by bands at 2820 and 2714 cm^{-1}, which were connected with the C—H stretching vibration of aldehyde groups. Moreover, the spectrum exhibited a band at 2170 cm^{-1}, which could have been related to C—O stretching vibrations from carbon monoxide.

From the literature,[3,24,50,51] it followed that decomposition of urethane linkages in an inert atmosphere can occur according to three basic mechanisms:

1. Dissociation to isocyanate and alcohol:

$$ArNHCOOR \rightarrow ArNCO + ROH$$

   The resulting isocyanate may then undergo the reaction of condensation at temperatures of 150–300°C with the formation of carbodiimides and carbon dioxide.
2. The formation of primary amine, alkenes, and carbon dioxide:

$$ArNHCOOCR_1R_2CH_2R_3 \rightarrow CR_1R_2{=}CHR_3 + ArNH_2 + CO_2$$

3. The formation of secondary amine and carbon dioxide in the case of the sudden heating of PUR (>300°C):[3]

$$ArNHCOOR \rightarrow ArNHR + CO_2$$

In view of the possibility of alcohol formation, according to mechanism 1, a TGA–FTIR analysis was also carried out for the unconventional chain extender, that is, diol E. From the FTIR spectrum

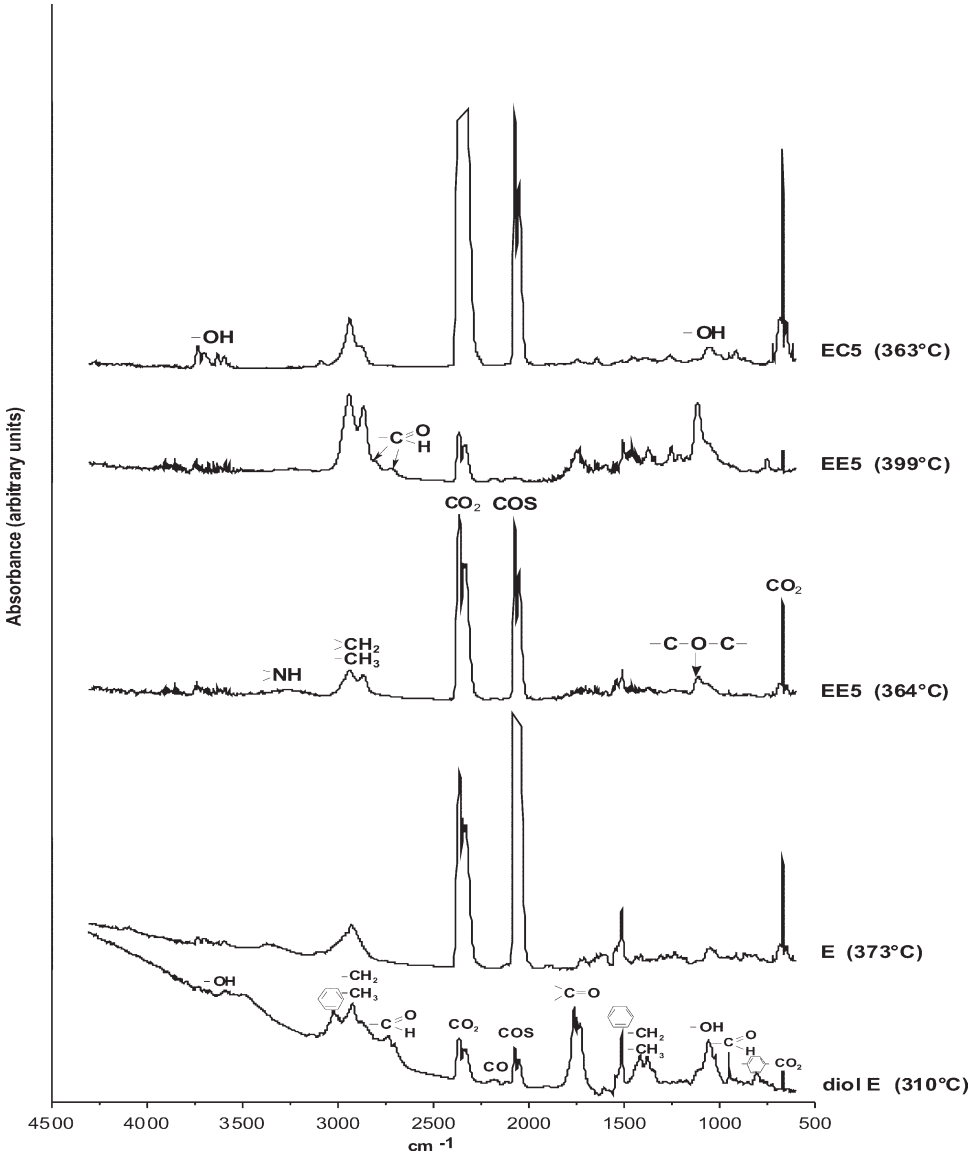

Figure 4 FTIR spectra of volatile products obtained at the maximum rate of mass loss of the thermal decomposition of diol E, (E) the regular PUR from diol E, and SPURs EC5 (for first stage) and EE5 (for first and second stages).

obtained at the maximum decomposition rate (310°C), presented in Figure 4, it appeared that the decomposition of diol E occurred with the emission of carbonyl sulfide, carbon dioxide, carbon monoxide, carbonyl compounds (including aldehydes), and alcohols.

The presence of carbon dioxide, amines, and alcohols, being the products of the decomposition of diol E in the volatile products of decomposition of the regular PUR, indicated that decomposition of urethane linkages may have taken place according to both mechanisms 1 and 2. On the other, hand the existence of carbonyl sulfide testified to the decomposition of sulfide linkages. In view of a much greater intensity of the band originating from carbonyl sulfide than from carbon dioxide, one should also consider the decomposition mechanism of urethane and sulfide linkages, which is not accompanied by the emission of carbon dioxide but only of carbonyl sulfide, as shown in Scheme 2.

At the first stage, a strongly nucleophilic sulfur atom, present in structure **I**, attacks the carbonyl group, and a transient structure is formed in the form of a five-membered ring (**II**), which at the next stage reorganizes into structure **III**. An attack of the oxide atom situated in an antiperiplanar manner in relation to the sulfur atom onto a carbon atom connected with the sulfur, occurring according to the mechanism of nucleophilic substitution, results in the formation of a thiourethane group and the emission of ethylene oxide. The decomposition of such a group at elevated temperature, occurring similarly to the decomposition of a urethane group (mechanism 3), is responsible for carbonyl sulfide formation. It is to be stressed

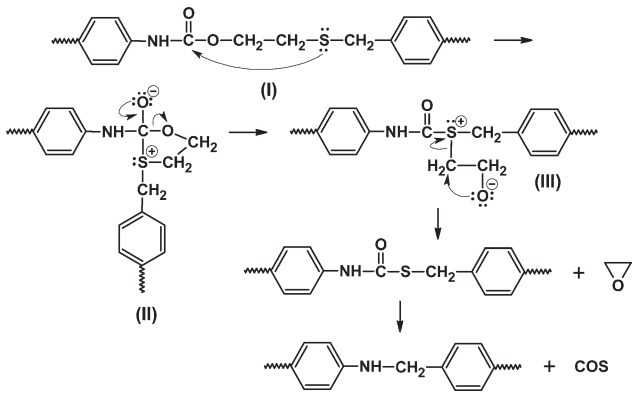

Scheme 2 Decomposition mechanism of the regular PUR based on diol E.

that apart from carbonyl sulfide, no other volatile sulfur compounds were found in the products of polymer decomposition.

In the case of polymer EE5, the first stage (364°C) was mostly characterized by the decomposition of the hard segment (emission of the same products as for the suitable regular PUR) and the beginning of the decomposition of the PTMO soft segment (the occurrence of the bands originating from the C—O stretching vibration of the ether group and the symmetric C—H stretching vibration of the methylene and methyl groups, which indicated the emission of aliphatic ethers). At the second stage (399°C), only the decomposition of the PTMO soft segment took place (no emission of carbonyl sulfide). Of course, at this stage, the decomposition of the unvolatile products obtained at the first stage occurred. The main volatile products of the decomposition of the PTMO soft segment were aldehydes and aliphatic ethers. The same compounds were detected by other authors in SPURs with PTMO soft segments and conventional hard segments.[52,53]

In the case of polymer EC5, the decomposition of the hard segment occurred simultaneously with the decomposition of the soft segment; this was confirmed by the much greater emission of carbon dioxide compared to that of carbonyl sulfide in the first stage (364°C) of decomposition. Because of the lack of the N—H stretching vibration band originating from amine groups, we supposed that the decomposition of urethane linkages in this case did not take place according to mechanism 2. The main volatile products of the decomposition of the PHCD soft segment were alcohols (a growth of the band intensity at 3690–3590 cm^{-1}, attributed to O—H stretching vibrations compared to the regular PUR) and not aldehydes and aliphatic ethers (absence of bands at 2830–2695 cm^{-1} connected with C—H stretching vibration from aldehyde groups and a very weak band at 1130 cm^{-1}, associated with C—O stretching vibration from ether groups), as was found for the decomposition of the PTMO soft segment.

XRD analysis

Considering the obtained DSC data (the lack of endothermic peaks on the thermograms of the PHCD-based SPURs, with the exception of EC2), we did the XRD analysis only for the PTMO-based polymers. The results of the analysis of the XRD patterns by the WAXSFIT program are presented in Table V

TABLE V
XRD Data of the PTMO-Based SPURs

PTMO component	2θ (°)			FWHM (°)			Area of diffraction peak (arbitrary units)		
	Diol component			Diol component			Diol component		
	E	P	H	E	P	H	E	P	H
E2	19.3	19.0	19.6	1.3	3.1	2.6	10	7	11
	19.8	20.3	19.9	5.8	8.1	6.5	100	100	100
	19.9		23.0	9.6		1.4	21		4
	21.9		25.7	8.8		4.1	45		12
E4	19.1	19.4	19.9	3.4	3.6	2.3	9	16	8
	20.1	20.3	20.0	8.1	7.7	6.6	100	100	100
	26.8		23.0	4.7		1.3	3		4
			25.9			3.9			11
E5	19.2	19.3	20.0	2.0	3.8	2.7	44	39	23
	20.2	20.5	20.1	7.3	7.4	6.6	100	100	100
			23.1			1.4			23
			26.0			3.6			23
E6	19.2	19.7	19.7	2.6	3.3	2.5	42	13	8
	20.2	20.5	20.0	7.3	8.0	7.4	100	100	100
			22.8			0.9			1
			26.2			3.0			6
E8	19.5	19.7	19.6	3.4	3.1	2.8	15	8	9
	20.1	20.2	20.1	8.2	7.5	7.8	100	100	100

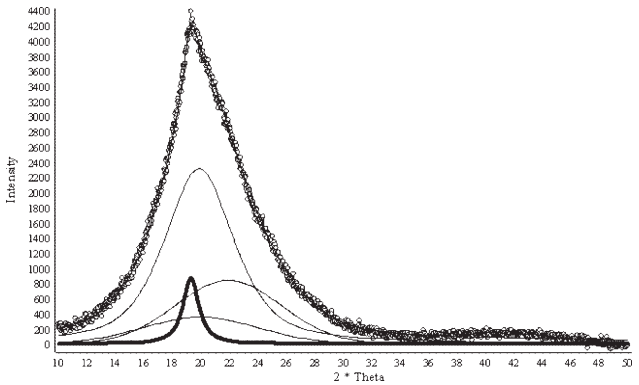

Figure 5 XRD curve (points) of SPUR EE2 resolved into crystalline (solid thick line) and amorphous peaks (solid thin lines).

and on a sample plot in Figure 5 (for polymer EE2). Moreover, the XRD patterns of all of the polymers obtained from diol H (HE2-8) and one polymer obtained from diol E (EE2) can be found in Figure 6.

The peaks originating from a crystalline phase [full width at half-maximum (FWHM) in the range

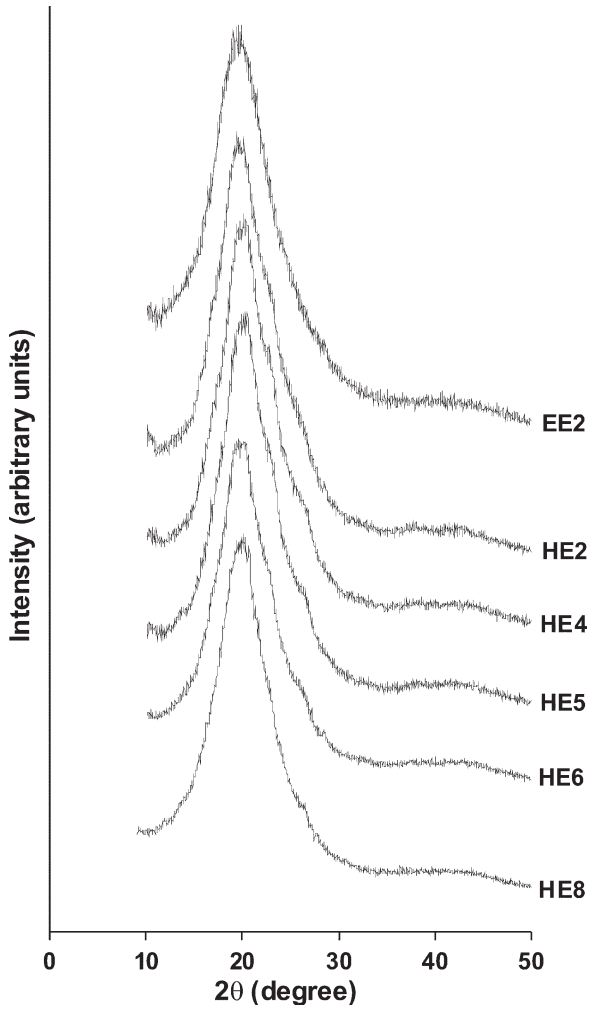

Figure 6 XRD patterns of the SPURs based on PTMO.

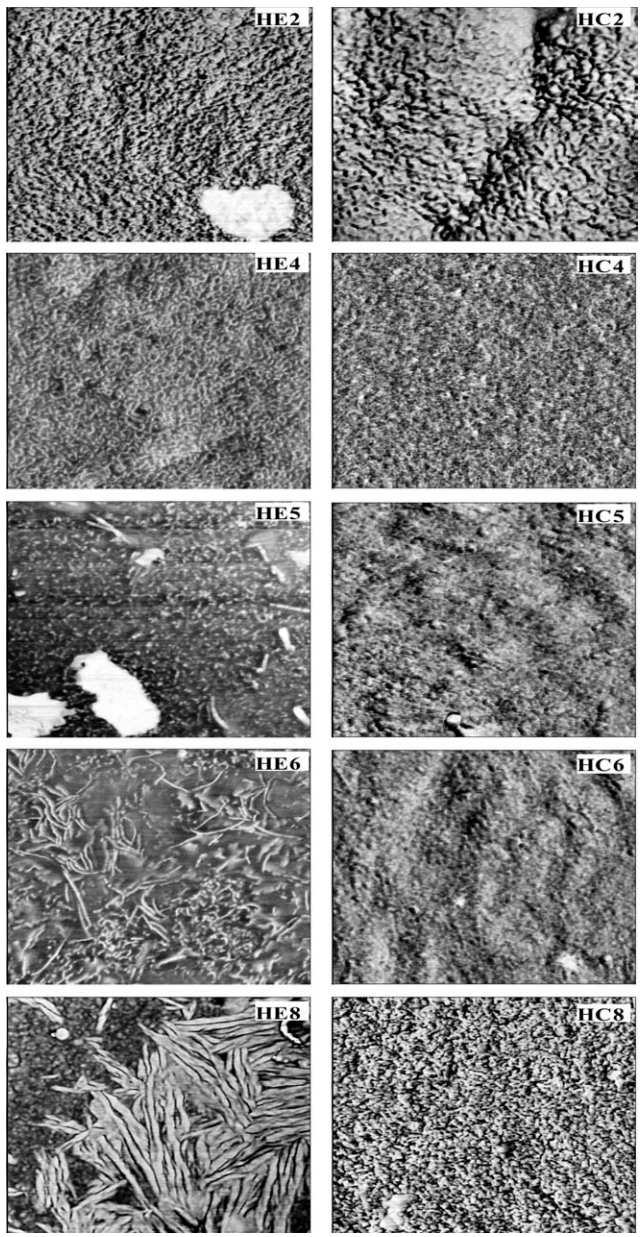

Figure 7 AFM phase images of films of the SPURs based on diol H and PTMO (left column) or PHCD (right column) at a 1-μm scan size.

0.9–1.4°] were only found on the XRD patterns of series HE (except for polymer HE8) and in polymer EE2. The received data correlated rather well with the DSC results. For series HE, together with the increase of the soft-segment content, T_m of the hard segment (with a higher temperature peak taken into account) decreased the least compared to those of the remaining series (see Table III and Fig. 2). This corresponded with the persistence of the crystalline phase in the polymers of this series. Moreover, in this series, the smallest difference was observed in T_m between the regular PUR obtained from diol H and the respective SPURs. In the remaining series, a significant decrease in T_m of the SPURs was

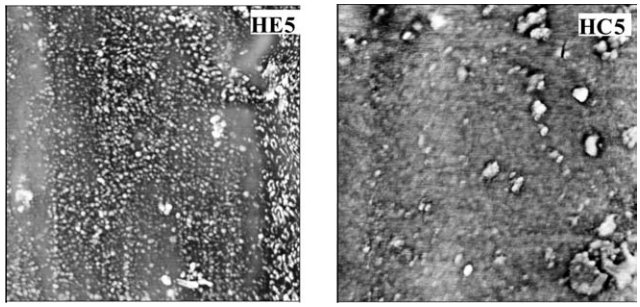

Figure 8 AFM phase images of the cuttings of SPURs HE5 and HC5 at a 1-μm scan size.

observed in comparison to the regular PURs, and the XRD data indicated an almost amorphous structure of these polymers. An exception was polymer EE2, which showed a T_m value close to that of the regular PUR obtained from diol E, and only in this polymer was the presence of a crystalline phase observed.

AFM

The main purpose of the AFM experiments was to study the surface morphology of the SPURs at the nanoscopic level. For these studies, the polymers based on diol H were chosen, with both the PTMO and PHCD soft segments because, for all of the polymers, it was possible to prepare cast films. The obtained phase images of all of these SPURs are given in Figure 7.

The images of the SPURs with the PTMO soft segment exhibited a two-phase morphology of all of the polymers. The observed dark areas corresponded to soft-segment domains, whereas the bright ones were associated with the presence of hard-segment domains. For sample HE2, at a hard-segment content of 75.6 wt %, hard-segment domains were a continuous phase (dark features dispersed in a bright matrix). For sample HE4 (56.9 wt % content of hard segments), a change in the image occurred, already clearly marked for sample HE5, where bright features dispersed in a dark matrix were observed. A phase inversion occurred here: the soft-segment domains became a continuous phase. Sample HE4 showed short hard-segment domains densely packed (uniformly distributed) in a soft-segment matrix. On the other hand, in sample HE5, there were also larger size single rodlike structures, which, in sample HE6, got significantly more numerous and displayed a tendency to form lamellar structures. Their width was about 10 nm, and their length approached about 250 nm. In sample HE8, with the lowest content of hard segments (30 wt %), the stacked lamellar structures were dominant.

In the case of the analogous PHCD-based SPURs, we saw little diversity in the appearance of the obtained AFM phase images. These polymers showed a relatively homogeneous surface, which pointed to their considerable degree of phase mixing. This was also confirmed by the high values of T_g, which were significantly different from the value received for PHCD. Such highly mixed-phase morphology could be caused by the formation of a strong hydrogen-bonding interaction between carbonate and urethane groups[25] and relatively less so by the molecular weight of the polycarbonate soft segment.[28]

The small diversity in the appearance of the obtained AFM phase images of the PHCD-based SPURs in comparison with the PTMO-based ones may additionally have been caused by the greater

TABLE VI
Mechanical Properties of the PTMO-Based SPURs and PUR Obtained Without the Use of a Chain Extender (PTMO+MDI)

Polymer	Hardness (Shore A/D)	Modulus of elasticity (MPa)	Tensile strength (MPa)	Elongation at break (%)	Pressing temperature (°C)
EE2	84/49	79.2	34.0	235	170
EE4	76/35	12.4	34.5	340	165
EE5	73/29	6.0	25.9	510	150
EE6	66/22	2.3	15.0	560	145
EE8	21/—	0.1	0.8	620	65
PE2	79/34	11.9	36.5	260	170
PE4	76/32	14.9	32.3	400	170
PE5	73/29	6.3	29.0	520	150
PE6	63/20	1.3	21.7	610	125
PE8	32/—	0.2	2.1	850	75
HE2	79/32	14.3	35.2	270	165
HE4	77/31	25.5	32.9	450	165
HE5	76/30	18.8	28.1	560	165
HE6	72/25	12.0	25.0	750	165
HE8	54/13	7.2	9.9	940	85
PTMO+MDI	30/—	0.6	0.3	100	90

TABLE VII
Mechanical Properties of the PHCD-Based SPURs and PUR Obtained Without the Use of a Chain Extender (PHCD+MDI)

Polymer	Hardness (Shore A/D)	Modulus of elasticity (MPa)	Tensile strength (MPa)	Elongation at break (%)	Pressing temperature (°C)
EC2	93/64	1047.9	55.8	30	160
EC4	91/53	530.5	42.0	250	160
EC5	81/29	35.5	42.6	260	160
EC6	70/23	2.5	42.9	340	165
EC8	63/20	0.4	9.6	525	145
PC2	94/65	967.3	59.6	45	160
PC4	93/49	242.6	42.2	250	170
PC5	79/29	7.4	44.4	315	165
PC6	68/24	1.7	34.1	350	145
PC8	64/21	0.4	7.5	575	145
HC2	92/57	644.6	38.9	250	160
HC4	77/30	5.1	39.7	275	160
HC5	69/26	1.9	46.7	350	145
HC6	67/25	0.8	22.6	425	145
HC8	65/22	0.5	14.8	525	135
PHCD+MDI	61/17	0.4	9.8	600	135

stiffness of the PHCD chains compared to the PTMO chains.

Moreover, the bulk morphology of the chosen samples HE5 and HC5 was examined. The obtained phase images, given in Figure 8, also pointed to the higher degree of phase mixing of the PHCD-based SPURs compared to the PTMO-based ones.

Mechanical properties

The Shore A/D hardness and tensile properties were determined for all of the SPURs and PURs obtained without a chain extender, and the results are shown in Tables VI and VII and Figures 9 and 10.

As is evident from the data presented in Tables VI and VII, the PHCD-based SPURs showed higher tensile strengths (7.5–59.6 vs 0.8–36.5 MPa) and lower elongations at break (45–575 vs 235–940%) than the corresponding PTMO-based ones. Most of the SPURs with the PHCD soft segment also exhibited higher hardness and modulus of elasticity values. Particularly high values of the modulus of elasticity (242.6–1047.9 MPa) and the highest values of hardness (>90A) were shown by polymers EC2, EC4, PC2, PC4, and HC2 with T_g's above 25°C. These polymers at 23°C, that is, at the temperature of the tensile test, showed plastic rather than elastomeric properties. The stress–strain curves of these SPURs exhibited yield stress, as shown in Figure 10 for sample HC2. Also, sample EE2, with a T_g of 26.3°C, was characterized by a relatively high modulus of elasticity (79.2 MPa) and the highest values of hardness (84 A) in the PTMO series. The stress–strain curve of this SPUR also showed yield stress. The remaining polymers, both of the PTMO and PHCD series, displayed typical elastomeric stress–strain curves with higher elongations (see Figs. 9 and 10 for the diol H-based SPURs). The differences in the mechanical properties between the polymers of the

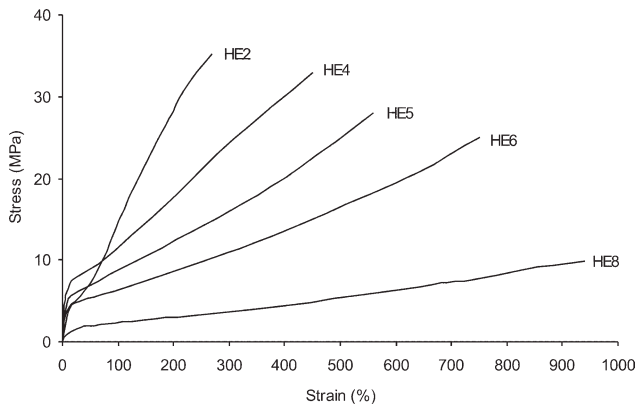

Figure 9 Stress–strain curves of the SPURs based on diol H and PTMO.

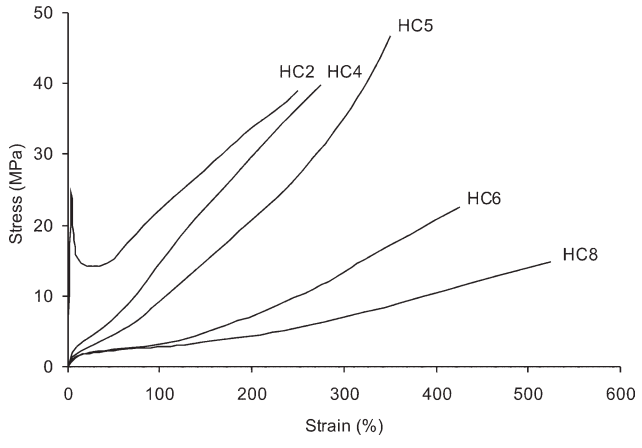

Figure 10 Stress–strain curves of the SPURs based on diol H and PHCD.

PTMO and PHCD series were caused by differences in intersegment hydrogen bonding between the hard and soft segments.

In each series of polymers, increased soft-segment contents resulted in decreased modulus of elasticity and hardness values and in an increased elongation at break. Generally, elongation increased in the following order of chain extender used: diol E < diol P < diol H. Among the polymers with 40–80 mol % PTMO contents, the highest modulus of elasticity and hardness values were found for those obtained from diol H and were characterized by the highest degree of ordering of hard-segment domains. Only these polymers showed a higher modulus than the analogous SPURs with the PHCD soft segment. Moreover, an increased soft-segment content caused a decrease in the tensile strength in the PTMO series (from $\sim$ 36 to $\sim$ 1 MPa). In the case of the PHCD series, this correlation was not observed, and polymers with the highest tensile strength, in the range of about 40 to 60 MPa, were obtained at 20–50 mol % (from diols P and H) and 20–60 mol % (from diol E) contents of the soft segment. The synthesized SPURs (except for EC8 and PC8) exhibited higher tensile strengths than the suitable PURs obtained without a chain extender.

A decisive majority of the obtained SPURs with 20–60 mol % contents of soft segments showed 2–4 times higher tensile strengths than their HDI-based analogs described earlier.[54,55]

CONCLUSIONS

New high-molecular-weight thermoplastic SPURs (on the basis of the determined η_{red} values) were prepared from PTMO or PHCD (soft segments), MDI, and diols E, P, and H (chain extenders) with a classical one-step melt polymerization. Depending on the kind and amount of soft segment and the kind of chain extender, these polymers showed elastomeric or plastic properties. The PTMO-based SPURs were characterized by much lower T_g's and a higher degree of microphase separation than the corresponding PHCD-based ones. In both types of SPURs, with the increase in the soft-segment content, a decrease in T_g was observed (up to -48.1 vs -1.4°C) as well as an increase in the microphase separation, with this influence being greater for the PTMO-based SPURs. Because of a much better microphase separation, the polymers with a PTMO soft segment showed some ordering in the hard-segment domains, and a crystalline phase was found through XRD analysis for the polymers HE2-6 and EE2.

The TGA results show that both in argon and air, the decomposition process of the SPURs occurred in several stages. A somewhat better thermal stability was exhibited by the PTMO-based SPURs compared to the PHCD-based ones. The newly obtained PTMO-based SPURs showed similar thermal stability to that of their analog on the basis of the conventional chain extender BD.[53] The TGA–FTIR analysis showed that the decomposition of the hard segment (derived from diol E) was mostly accompanied by the emission of carbonyl sulfide and carbon dioxide; the PTMO soft segment decomposed into aldehydes and aliphatic ethers, and the PHCD soft segment decomposed into carbon dioxide and alcohols.

In general, the PHCD-based SPURs showed higher tensile strengths (up to 59.6 vs 36.5 MPa), hardnesses (up to 94 vs 84 A), and moduli of elasticity and lower elongations at break than the corresponding PTMO-based ones. In each series, the increased soft-segment content resulted in a decreased modulus of elasticity and hardness and an increased elongation at break.

The PTMO-based SPURs discussed in this article, with hardnesses in the range 73–79 A, showed similar or higher tensile strengths to their commercial analog PTMO/MDI/BD, that is, Pellethane 2363-80AE (29.0 MPa).[56] However, the PHCD-based SPURs, with elastomeric properties and hardnesses in the range 69–81 A, exhibited similar tensile strengths to those of their commercial analogs with an MDI/BD hard segment and a poly(hexane-1,6-diylethylene carbonate) diol soft segment, that is, Bionate 80A and ChronoFlexAR 75A (46.6 and 51.7 MPa, respectively).[56]

References

1. Ulrich, H. In Encyclopedia of Polymers Science and Technology, 3rd ed.; Mark, H. F., Ed.; Wiley: Hoboken, NJ, 2003; Vol. 4.
2. Holden, G. In Kirk-Othmer Encyclopedia of Chemical Technology, 5th ed.; Kroschwitz, J., Ed.; Wiley-Interscience: New York, 2007; Vol. 24.
3. Wirpsza, Z. Polyurethanes: Chemistry, Technology and Applications; Ellis Horwood: New York, 1993.
4. Stokes, K. J Biomater Appl 1988, 3, 228.
5. Tanzi, M. C.; Mantovani, D.; Petrini, P.; Guidoin, R.; Laroche, G. J Biomed Mater Res 1997, 36, 550.
6. Pawłowski, P.; Rokicki, G. Polymer 2004, 45, 3125.
7. Khan, I.; Smith, N.; Jones, E.; Finch, D. S.; Cameron, R. E. Biomaterials 2005, 26, 621.
8. Tang, Y. W.; Labow, R. S.; Santerre, J. P. J Biomed Mater Res 2001, 57, 597.
9. Anderson, J. M.; Hiltner, A.; Wiggins, M. J.; Schubert, M. A.; Collier, T. O.; Kao, J. K.; Mathur, A. B. Polym Int 1998, 46, 163.
10. Mathur, A.; Collier, T.; Kao, W.; Wiggins, M.; Schubert, M.; Hiltner, A.; Anderson, J. J Biomed Mater Res 1997, 36, 246.
11. Fare, S.; Petrini, P.; Motta, A.; Cigada, A.; Tanzi, M. J Biomed Mater Res 1999, 45, 62.
12. Christenson, E. M.; Dadsetan, M.; Wiggins, M.; Anderson, J. M. J Biomed Mater Res A 2004, 69, 407.
13. Salacinski, H.; Tai, N.; Carson, R.; Edwards, A.; Hamilton, G.; Seifalian, A. J Biomed Mater Res 2002, 59, 207.
14. Salacinski, H.; Odlyha, M.; Hamilton, G.; Seifalian, A. Biomaterials 2002, 23, 2231.

15. Christenson, E. M.; Anderson, J. M.; Hiltner, A. J Biomed Mater Res A 2006, 76, 480.
16. Stokes, K.; McVenes, R.; Anderson, J. M. J Biomater Appl 1995, 9, 321.
17. Capone, C. D. J Biomater Appl 1992, 7, 108.
18. Szycher, M.; Reed, A.; Potter, J. J Biomater Appl 1994, 8, 210.
19. Gogolewski, S. Colloid Polym Sci 1989, 267, 757.
20. Zdrahala, R. J. J Biomater Appl 1996, 11, 37.
21. Rokicki, G.; Kowalczyk, T. Polymer 2000, 41, 9013.
22. Gunatillake, P. A.; Meijs, G. F.; McCarthy, S. J.; Adhikari, R.; Sherriff, N. J Appl Polym Sci 1998, 69, 1621.
23. Tang, Y. W.; Labow, R. S.; Santerre, J. P. J Biomed Mater Res 2001, 56, 516.
24. Chattopadhyay, D. K.; Webster, D. C. Prog Polym Sci 2009, 34, 1068.
25. Martin, D. J.; Meijs, G. F.; Renwick, G. M.; Gunatillake, P. A.; McCarthy, S. J. J Appl Polym Sci 1996, 60, 557.
26. Lee, D. K.; Tsai, H. B.; Tsai, R. S.; Chen, P. H. Polym Eng Sci 2007, 47, 695.
27. Chang, C. C.; Chen, K. S.; Yu, T. L.; Chen, Y. S.; Tsai, C. L.; Tseng, Y. H. Polym J 1999, 31, 1205.
28. Eceiza, A.; Martin, M. D.; de la Caba, K.; Kortaberria, G.; Gabilondo, N.; Corcuera, M. A.; Mondragon, I. Polym Eng Sci 2008, 48, 297.
29. Li, F. K.; Hou, J. N.; Zhu, W.; Zhang, X.; Xu, M.; Luo, X. L.; Ma, D. Z.; Kim, B. K. J Appl Polym Sci 1996, 62, 631.
30. Zia, K. M.; Barikani, M.; Zuber, M.; Bhatti, I. A.; Bhatti, H. N. Iran Polym J 2008, 17, 61.
31. Tocha, E.; Janik, H.; Debowski, M.; Vancso, G. J. J Macromol Sci Phys 2002, 41, 1291.
32. Padmavathy, T.; Srinivasan, K. S. V. J Macromol Sci Polym Rev 2003, 43, 45.
33. Wang, H. H.; Yuen, U. E. J Appl Polym Sci 2006, 102, 607.
34. Son, T. W.; Lee, D. W.; Lim, S. K. Polym J 1999, 31, 563.
35. Zhang, C.; Zhang, N. J Biomed Mater Res Part B: Appl Biomater 2006, 79, 335.
36. Tatai, L.; Moore, T. G.; Adhikari, R.; Malherbe, F.; Jayasekara, R.; Griffiths, I.; Gunatillake, P. A. Biomaterials 2007, 28, 5407.
37. Liaw, D. J. J Appl Polym Sci 1997, 66, 1251.
38. Rogulska, M.; Kultys, A.; Podkościelny, W. Eur Polym J 2007, 43, 1402.
39. Hong, J. L.; Lillya, C. P.; Chien, J. C. W. Polymer 1992, 33, 4347.
40. Woo, E. J.; Farber, G.; Farris, R. J.; Lillya, C. P.; Chien, J. C. W. Polym Eng Sci 1985, 25, 834.
41. Hsu, S.; Kao, Y. Macromol Biosci 2005, 5, 246.
42. Duda, A.; Penczek, S. In Encyclopedia of Polymers Science and Technology, 2nd ed.; Mark, H. F., Ed.; Wiley: Hoboken, NJ, 1989; Vol. 16.
43. Kultys, A. In Encyclopedia of Polymers Science and Technology, 3rd ed.; Mark, H. F., Ed.; Wiley: Hoboken, NJ, 2003; Vol. 4.
44. Kultys, A.; Podkościelny, W.; Majewski, W. J Polym Sci Part A: Polym Chem 2000, 38, 1767.
45. Rabiej, M.; Rabiej, S. Analiza Krzywych Dyfrakcyjnych Polimerów za Pomocą Programu Komputerowego WAXSFIT; ATM: Bielsko-Biała, Poland, 2006.
46. Xu, Y.; Petrovic, Z.; Das, S.; Wilkes, G. L. Polymer 2008, 49, 4248.
47. Bajsic, E. G.; Rek, V.; Agic, A. J Elastom Plast 2003, 35, 311.
48. Bajsic, E. G.; Rek, V. J Appl Polym Sci 2001, 79, 864.
49. Dunn, J. G.; Chamberlain, A. C.; Fisher, N. G.; Avraamides, J. J Therm Anal 1997, 49, 1399.
50. Simon, J.; Barla, F.; Kelemen-Haller, A.; Farkas, F.; Kraxner, M. Chromatographia 1988, 25, 99.
51. Shufen, L.; Zhi, J.; Kaijun, Y.; Shuqin, Y.; Chow, W. K. Polym-Plast Technol 2006, 45, 95.
52. Cervantes-Uc, J. M.; Moo Espinosa, J. I.; Cauich-Rodrıguez, J. V.; Avila-Ortega, A.; Vazquez-Torres, H.; Marcos-Fernandez, A.; San Roman, J. Polym Degrad Stab 2009, 94, 1666.
53. Herrera, M.; Matuschek, G.; Kettrup, A. Polym Degrad Stab 2002, 78, 323.
54. Kultys, A.; Pikus, S. J Polym Sci Part A: Polym Chem 2001, 39, 1733.
55. Kultys, A.; Rogulska, M.; Pikus, S.; Skrzypiec, K. Eur Polym J 2009, 45, 2629.
56. MatWeb. http://www.matweb.com.